

Journal of Hydrology

Examining the outstanding Euro-Mediterranean drought of 2021-2022 and its historical context --Manuscript Draft--

Manuscript Number:	
Article Type:	Research paper
Keywords:	Climate extreme; SPEI; Atmospheric evaporative demand; Atmospheric circulation; climate change; global warming
Corresponding Author:	J.M. Garrido-Perez Universidad Complutense de Madrid Madrid, Comunidad de Madrid SPAIN
First Author:	J.M. Garrido-Perez
Order of Authors:	J.M. Garrido-Perez Sergio M. Vicente-Serrano David Barriopedro Ricardo García-Herrera Ricardo Trigo Santiago Beguería
Abstract:	<p>The Euro-Mediterranean region experienced a remarkable drought during the hydrological year 2021/22. Substantial and widespread impacts on water supply systems, agricultural crops, and the production of hydroelectric power were observed. This assessment characterises the drought from a long-term perspective using a multi-index approach and analyses the associated atmospheric circulation at the annual and monthly time scales. The main dynamical forcing of the drought was the unusual recurrence of high-pressure systems over western Europe, at least partly due to an anomalous southward shift in blocking activity and a remarkable occurrence of low-latitude blocks. This led to record-breaking positive geopotential height anomalies over western Europe and a poleward displacement of the North Atlantic eddy-driven jet. Although most of the region was affected by mild drought conditions, the 2021/22 event was not unprecedented in terms of precipitation deficits since other periods of the 20th century (e.g., in the 1920s, 1940s and 1970s) displayed moderate and severe drought conditions over larger areas. However, the 2021/22 drought has been the most intense since at least 1891 because of high atmospheric evaporative demand (AED) values associated with extreme temperatures, especially during the summer of 2022. This enhanced AED also contributed to depleting soil moisture and reducing runoff generation, leading to unprecedented deficits since at least 1965. Finally, we find important differences in the 2021/22 event as compared to other major historical droughts over the Euro-Mediterranean region. In particular, the contrasting effect of AED evidences its increasing role over the last decades and warns about the current risk of experiencing unprecedented droughts.</p>
Suggested Reviewers:	<p>Davide Faranda Laboratory for Sciences of Climate and Environment davide.faranda@cea.fr Expert knowledge of climate dynamics and climate extremes. He published an attribution study of the 2021/22 drought.</p> <p>Dominik L. Schumacher ETH Zurich Institute for Atmospheric and Climate Science dominik.schumacher@env.ethz.ch Expert knowledge of land-atmosphere interactions and extreme weather events. He has a preprint about an attribution study of the 2021/22 drought.</p> <p>Sigrid J. Bakke University of Oslo s.j.bakke@geo.uio.no</p>

	<p>Expert knowledge about hydrology extremes and droughts. Author of some peer-reviewed publications about precedent European droughts and a preprint about the relationship between atmospheric circulation and droughts in Europe.</p>
	<p>Monica Ionita Alfred Wegener Institute for Polar and Marine Research monica.ionita@awi.de Expert knowledge of climate research and environmental physics. Author of a number of peer-reviewed publications about precedent European droughts contextualized in the long-term.</p>
	<p>Ondřej Lhotka Institute of Atmospheric Physics Czech Academy of Sciences lhotka.o@czechglobe.cz Expert knowledge of land-atmosphere coupling, climate models and atmospheric circulation. Author of a number of peer-reviewed publications about precipitation variability in Europe.</p>

1 **Examining the outstanding Euro-Mediterranean drought of 2021-2022 and its**
2 **historical context**

3 Jose M. Garrido-Perez¹, Sergio M. Vicente-Serrano², David Barriopedro³, Ricardo García-
4 Herrera^{1,3}, Ricardo Trigo^{4,5}, Santiago Beguería⁶

5 ¹Dpto. Física de la Tierra y Astrofísica, Universidad Complutense de Madrid, Madrid,
6 Spain

7 ²Instituto Pirenaico de Ecología (IPE), CSIC, Zaragoza, Spain

8 ³Instituto de Geociencias (IGEO), CSIC-UCM, Madrid, Spain

9 ⁴Instituto Dom Luiz, Faculdade de Ciências da Universidade de Lisboa, Lisboa, Portugal

10 ⁵Departamento de Meteorologia, Universidade Federal do Rio de Janeiro, Rio de Janeiro,
11 Brazil

12 ⁶Estación Experimental de Aula Dei - Consejo Superior de Investigaciones Científicas
13 (EEAD-CSIC), Zaragoza, Spain.

14 Corresponding author: (josgarri@ucm.es)

15 **Keywords:** Climate extreme; SPEI; Atmospheric evaporative demand; Atmospheric
16 circulation; Climate change; Global warming

17

18 **1. Introduction**

19 The 2022 European State of the Climate Report highlights that the climate in
20 Europe during that year was marked by a widespread drought. Starting from winter
21 2021/22, there was a persistent deficit of precipitation, resulting in pronounced negative
22 anomalies in soil moisture and streamflow over a large area of the continent (Copernicus,
23 2023). The drought had far-reaching consequences for numerous sectors, including
24 agriculture, energy, river transport, and natural systems (Toreti et al., 2022, and references
25 therein). Cereal crop production in 2022 was 9 percent below the previous five-year
26 average in the European Union (FAO, 2022). The level of hydropower generation across
27 Europe was the lowest since at least 2000 (Jones et al., 2023). The number of detected fires
28 reached the highest level in the European Forest Fire Information System data record,
29 which started in 2006 (Sundström et al., 2022).

30 Since the beginning of the 21st century, Europe has experienced a series of droughts
31 associated with precipitation deficits (Fink et al., 2004; Santos et al., 2007; Kendon et al.,
32 2013; Spinoni et al., 2015a; Van Lanen et al., 2016; Ionita et al, 2017; Laaha et al., 2017;
33 García-Herrera et al., 2019; Oikonomou et al., 2020; Peters et al., 2020). Moreover, drought
34 severity has worsened across extensive areas of southern and central Europe during the last
35 decades (Spinoni et al., 2015b; 2017; Stagge et al., 2017). This drying trend has been linked
36 mainly to increases in temperature and record-breaking heatwaves associated with climate
37 change (Seneviratne et al., 2021). Regional warming enhances atmospheric evaporative
38 demand (AED), accelerating the rate of water loss from water bodies, soil and natural
39 vegetation (Seneviratne et al., 2021), and intensifying the water stress of crops and
40 ecosystems under dry conditions (Vicente-Serrano et al., 2020).

41 In addition to land-atmosphere feedbacks, the increasing drought severity over
42 certain European regions has also been related to changes in the frequency of large (and
43 synoptic) scale atmospheric circulation patterns (Ionita et al., 2020; Lhotka et al., 2020;
44 Bakke et al., 2023), which exert a strong influence on moisture fluxes and precipitation
45 (Kingston et al., 2015; Sousa et al., 2018). In this sense, the 2021/22 European drought
46 featured persistent high-pressure weather systems over western Europe (Copernicus, 2023).
47 Although some studies have already highlighted the key role of these synoptic conditions in
48 the drought event (Bakke et al., 2023; Faranda et al., 2023), a detailed study of the
49 associated atmospheric circulation and its temporal evolution has not been carried out so
50 far.

51 A couple of attribution studies have shown the role of human-induced climate
52 change in exacerbating the 2021/22 Euro-Mediterranean drought. While Faranda et al.
53 (2023) quantified the contribution of climate change on a standardized precipitation-AED
54 index by comparing circulation analogues of past (when global warming was absent) and
55 present periods, Schumacher et al. (2023) employed a statistical approach based on
56 observation-driven soil moisture estimates and climate models. In this work, we use four
57 standardized drought indices based on precipitation, precipitation-AED, soil moisture, and
58 runoff to perform an assessment of the 2021/22 drought event and contextualise it from a
59 long-term perspective. Given the reported regional divergences in the likelihood and
60 intensity trends of droughts over Europe as measured by different indices (Spinoni et al.,
61 2015b; Stagge et al., 2017; Gudmundsson et al., 2017), this multi-index approach allows us
62 to better frame the degree of exceptionality of the 2021/22 drought event in the historical
63 context.

64 The main objectives of this paper are threefold, namely: i) to characterise the
65 severity, evolution, and spatial extension of the 2021/22 Euro-Mediterranean drought for
66 different drought indices; ii) to put the drought event into a long-term context, including a
67 comparative analysis with previous extreme droughts at continental scale since 1891, and
68 iii) to investigate the associated atmospheric circulation through the analysis of specific
69 weather systems covering a wide range of spatial and temporal scales.

70 **2. Data and methods**

71 **2.1. Drought data and indices**

72 The 2021/22 drought and the historical evolution of drought severity are analysed
73 over the Euro-Mediterranean domain, defined as [15°W–32°E, 30°N–62°N] (red box in
74 Figure S1). We have generated drought indices from two data sources, based on reanalysis
75 and observational products, respectively, which are described in the following subsections.
76 The former is employed to characterise the 2021/22 drought using high-resolution data and
77 different drought indices for the 1965–2022 period, whereas the latter provides a much
78 longer record (1891–2022) to assess long-term trends and the exceptionality of the 2021/22
79 episode in the historical context. In both cases, drought severity is quantified with the
80 Standardised Precipitation Evapotranspiration Index (SPEI) (Vicente-Serrano et al., 2010),
81 which is defined as the normalised difference between precipitation and the AED. We also
82 compute a version of the SPEI considering AED constant (SPEI_c hereafter) in order to
83 isolate the role of precipitation on drought severity and to determine the influence of the
84 AED on the 2021/22 drought, which can be estimated as the difference between SPEI and
85 the SPEI_c. The monthly climatology of AED employed to calculate the SPEI_c was obtained

86 from the 1965–2022 reference period. The SPEI and SPEIc are computed at the time scales
87 of 1- and 12-months for each grid cell and the entire Euro-Mediterranean domain. For
88 coherence with the definition of hydrological year (defined as the 12-month period between
89 October and September), most of the analyses with the drought indices will be carried out
90 at 12-month time scales, unless stated otherwise. The gridded SPEI and SPEIc are
91 employed to characterise the spatial patterns and determine the surface area affected by
92 different levels of drought severity: mild ($\text{SPEI} \leq -0.85$, a return period of 1 in 5 years),
93 moderate ($\text{SPEI} \leq -1.28$, a return period of 1 in 10 years) and severe ($\text{SPEI} \leq -1.65$, a return
94 period of 1 in 20 years) (Agnew, 2000). The Euro-Mediterranean regional SPEI is obtained
95 from the spatial average values of the basic fields rather than by averaging the local SPEI
96 values.

97 ***2.1.1 ERA-land reanalysis***

98 We used monthly means of the following variables for the 1965–2022 period of the
99 ERA-land dataset (Muñoz-Sabater et al., 2021) at $0.1^\circ \times 0.1^\circ$ horizontal resolution:
100 precipitation, maximum and minimum air temperature, relative humidity, solar radiation,
101 wind speed, surface runoff and total column soil moisture. Meteorological data have only
102 been considered since 1965 because of inhomogeneities in the precipitation series before
103 that year (not shown). There are different procedures to estimate the AED, but the most
104 realistic ones are those that account for both the radiative and aerodynamic terms.
105 Accordingly, the ERA-land SPEI relies on the AED values inferred from the FAO-56
106 Penman-Monteith equation (Allen et al., 1998).

107 We also derived two additional standardised drought indices based on ERA-land
108 surface runoff and total column soil moisture, respectively. As the probability distribution

109 of these variables is not well defined, we followed the methodology of Vicente-Serrano et
110 al., (2012): for each grid point and monthly series, this approach selects the most suitable
111 probability distribution among ten candidates, based on the Shapiro-Wilks test of normality
112 (Stagge et al. 2015). These two drought indices were subsequently standardised using the
113 same procedure as for the SPEI. They are employed to quantify the surface affected by
114 mild, moderate and severe drought conditions, which are defined from the threshold values
115 corresponding to the abovementioned return periods (5, 10 and 20 years, respectively).

116 ***2.1.2 Observational products***

117 The historical SPEI (1891–2022) does not rely on AED values retrieved from the
118 FAO-56 Penman Monteith equation due to the unavailability of relative humidity, solar
119 radiation and wind speed for that period. Instead, it is calculated using monthly
120 precipitation from the GPCP dataset (Schneider et al., 2014), and empirical AED equations
121 based on maximum and minimum air temperature from the Berkeley land and ocean
122 temperature dataset (Rohde and Hausfather, 2020), both at 1° spatial resolution. This
123 simplified approach does not account for the whole aerodynamic and radiative terms in
124 AED, yielding more uncertain estimations of the SPEI (Vicente-Serrano et al., 2020). To
125 reduce this uncertainty, the AED was taken as the arithmetic mean of three estimates
126 derived from different empirical equations: the Hargreaves-Samani (Hargreaves and
127 Samani, 1985), the Bladney-Criddle (Blaney and Criddle, 1950) and the Kharrufa
128 (Kharrufa, 1985) methods. This historical AED series compares well with the Version 4
129 AED dataset (1901–2021) from the Climatic Research Unit (CRU), which applies a
130 simplified Penman-Monteith equation with constant wind speed (Harris et al., 2020). Our
131 procedure was also validated with ERA-land data by comparing the empirical AED

132 estimates based on temperature data with the more realistic series obtained from the FAO-
133 56 Penman-Monteith equation in subsection 2.1.1 (Figure S2). The parameters of the log-
134 logistic distribution employed to calculate the historical SPEI were obtained from the
135 1965–2022 reference period, which allows a fair comparison with the drought indices
136 derived from the ERA-land dataset. For all datasets and methods considered, we obtained a
137 similar evolution of the Euro-Mediterranean SPEI, which suggests that these empirical
138 approaches reproduce well the long-term evolution of the AED and that its variability is
139 mostly controlled by air temperature.

140 **2.2. Atmospheric circulation characterisation**

141 Three synoptic descriptors are examined to characterise the Euro-Atlantic
142 circulation during the 2021–2022 drought event: weather regimes (WRs), the North-
143 Atlantic eddy-driven jet (EDJ) and blocking events. They have been computed using daily
144 geopotential height at 500 hPa (Z500; WRs and blocking events) and zonal wind at 925–
145 700 hPa (North Atlantic EDJ) obtained for the 1940–2022 period of the ERA5 reanalysis
146 (Hersbach et al., 2020).

147 **2.2.1. Weather regimes**

148 To describe the large-scale flow patterns over the North Atlantic-European sector,
149 we have employed eight year-round WRs previously introduced in the context of wind
150 power (Garrido-Perez et al., 2020) and air quality (García-Herrera et al., 2022). These
151 recurrent patterns of atmospheric circulation were extracted from the climatological period
152 1981–2010 by applying a k-means clustering algorithm to area-weighted anomalies of daily
153 Z500 over the [30°W–25°E, 30°N–65°N] domain (blue box in Figure S1). Although the

154 classical WR framework over the Euro-Atlantic sector comprises four regimes (e.g.,
155 Michelangeli et al., 1995; Cassou, 2008; Ayarzagüena et al., 2018), these are seasonally
156 dependent and have mainly been applied to the winter season. The increase in the number
157 of WRs allows us to capture recurrent large- scale flow patterns all year-round and their
158 seasonal variability (Grams et al., 2017).

159 In this work, each day has been classified into one of these eight WRs based on the
160 minimum Euclidean distance of the daily Z500 anomaly fields (computed as the differences
161 of each daily value and the climatological 15-day running means for the corresponding
162 calendar day in 1981–2010) to the eight centroids (defined as the average Z500 anomaly for
163 all the days with a specific WR during the 1981–2010 period).

164 Figures S3-S5 display the Z500, temperature (for summer) and precipitation
165 anomaly composites for each WR during the 1981–2010 period. Full details of the
166 methodology and a brief overview of the main features of each WR can be found in
167 Sections 2.2 and S4 of Garrido-Perez et al. (2020).

168 **2.2.2. North Atlantic eddy-driven jet**

169 The detection of the North Atlantic EDJ is obtained from the low-pass zonal wind at
170 925–700 hPa over the [120°W–60°E, 15°N–75°N] domain (green box in Figure S1), as
171 described in Barriopedro et al. (2022). For the EDJ characterisation, here we use the
172 following three daily parameters:

- 173 - Latitudinal position: latitude where the zonal wind averaged over the North Atlantic
174 sector [60°W–0°E] is maximum
- 175 - Intensity: zonal wind at the latitudinal position

176 - Eastward extension: easternmost longitude of the EDJ, an indicator of the maximum
177 decrease in EDJ intensity over the eastern half of the domain

178 By extending the detection of the EDJ parameters to other longitudinal sectors, this
179 method also provides a 2-D gridded binary field that identifies the latitudes of the EDJ core
180 for each longitude and day. These daily snapshots are employed in this work to compute
181 anomaly frequency maps of the EDJ in order to analyse its structure during the 2021/22
182 drought event. Full details of the methodology can be found in Barriopedro et al. (2022).

183 **2.2.3. Blocking index**

184 Following Woollings et al. (2018), we identify blocking using the absolute (ABS)
185 method, which is an adaptation of that proposed by Davini et al. (2012). The ABS method
186 detects blocks when several conditions based on meridional Z500 gradients are fulfilled,
187 including a large-scale flow reversal at the mid-latitudes [45°N–70°N]. This method
188 guarantees the detection of large-scale, quasi-stationary and persistent patterns as it imposes
189 conditions of minimum extension, spatial overlapping between the blocked areas of
190 successive days and a minimum duration of 5 days. Additional analyses performed using
191 other blocking methods included in Woollings et al. (2018) indicate that the results
192 presented in this work are not very sensitive to the choice of the blocking index (not
193 shown).

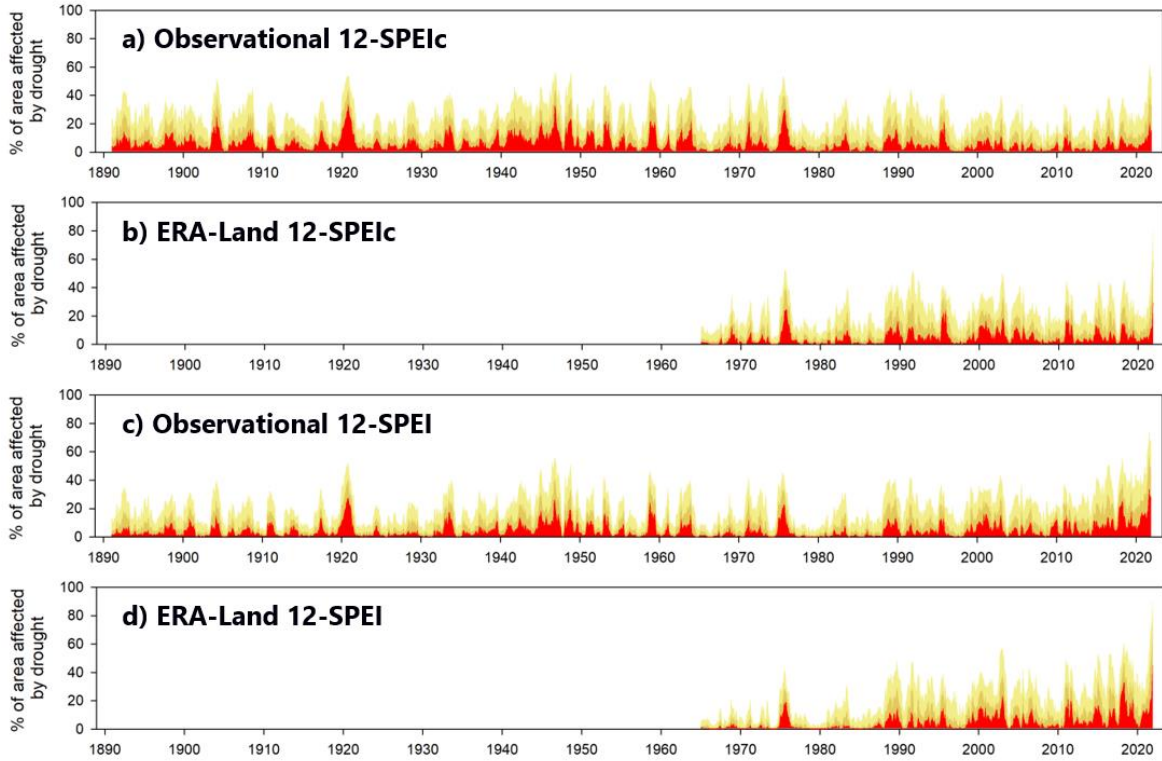
194 **3. Results**

195 **3.1. Long-term assessment of the 2021/22 drought event**

196 The evolution of the percentage of Euro-Mediterranean land areas affected by mild,
197 moderate, and severe drought conditions based on 12-SPEIc (Figure 1a-b) and 12-SPEI

198 (Figure 1c-d) in the historical (observations during 1891–2022; Figures 1a and 1c) and
199 recent (ERA-land reanalysis during 1965–2022; Figures 1b and 1d) periods is shown in
200 Figure 1. We first focus on the SPEIc, which represents the drought severity when
201 precipitation is only accounted for (i.e. disregarding the AED effects). The 2021/22 event
202 reached during the 12-month interval from December 2021 to November 2022 the largest
203 percentage of area affected by mild (80.7%), moderate (59.3%) and severe (29.6%) drought
204 for the 1965–2022 recent period based on the ERA-Land 12-SPEIc (Figure 1b). However,
205 in a longer historical context, the 2021/22 drought was not unprecedented. Other periods of
206 the 20th century displayed moderate and severe drought conditions over larger areas than
207 the 2021/22 drought when we consider the observational 12-SPEIc (e.g., in the 1920s,
208 1940s and 1970s; see Figure 1a). Despite this, the surface area affected by mild drought in
209 2021/22 has been the largest since at least 1891 (60.8% from September 2021 to August
210 2022). This long-term study allows us to contextualise the 2021/22 drought event: although
211 more than half of the Euro-Mediterranean region experienced mild drought conditions, the
212 surface area recording moderate and severe precipitation deficits was not unprecedented.

213

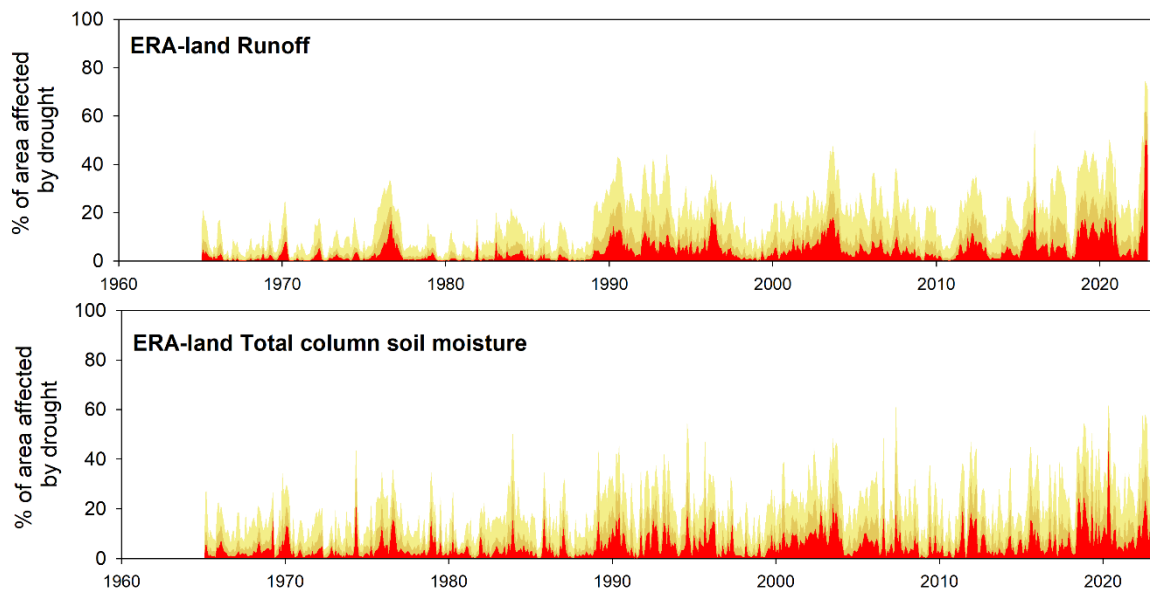


214

215 **Figure 1.** Evolution of the surface area affected by drought using the 12-SPEIc (a,b) and
 216 12-SPEI (c,d) from GPCP precipitation and Berkeley temperature (1891–2020) (a,c) and
 217 the ERA-land dataset (1965–2022) (b,d). Red: area affected by severe drought, Orange:
 218 moderate drought and yellow: mild drought.

219 A different rank is obtained when we examine the evolution of the SPEI (Figure 1c-
 220 d). The 2021/22 year was characterised by exceptionally large AED values, which were
 221 driven by the warm conditions recorded. Therefore, when the AED effects are added up to
 222 those of the precipitation deficits, the Euro-Mediterranean drought of 2021/22 turns out to
 223 be the most severe since at least 1891. In terms of the area affected, it reached the largest
 224 SPEI values during the 12-month interval from September 2021 to August 2022 for mild
 225 (73.6%), moderate (56.6%) and severe (33.6%) drought (Figure 1c).

226 The exceptional drought severity is confirmed by analysing the monthly soil
227 moisture and runoff deficits (Figure 2). Although the very intense precipitation deficits
228 recorded in 2021/22 were not as high as those reached during other major drought events
229 during the historical period (1891–2022), the surface area with moderate and severe runoff
230 and soil moisture deficits was exceptionally large, with no precedents in runoff since at
231 least 1965. In fact, 74.4%, 61.6% and 47.3% of the Euro-Mediterranean region was
232 affected respectively by mild, moderate and severe hydrological drought in September 2022
233 (Figure 2, bottom panel). This marked surface water imbalance is well explained by the
234 SPEI since the enhanced AED associated with extremely high temperatures contributed to
235 depleting soil moisture and reducing runoff generation.

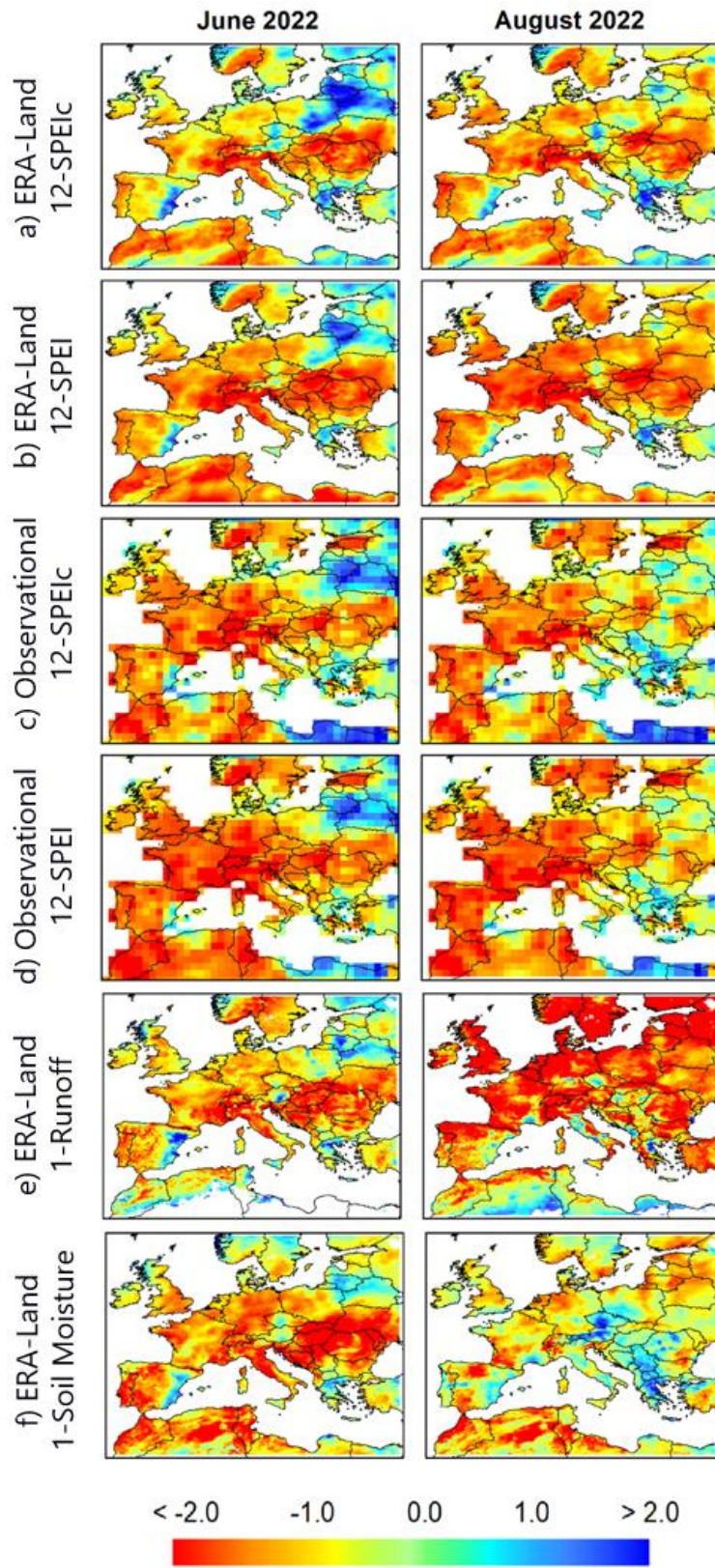


236 **Figure 2.** Monthly evolution of the surface area affected by drought using the 1-month
237 standardised runoff (top) and total column soil moisture (bottom) from the ERA-land
238 dataset (1965–2022). Red: area affected by severe drought, Orange: moderate drought and
239 yellow: mild drought.
240

241 The key role of AED in the extreme character of the 2021/22 event is also illustrated in
242 Figure 3, which shows the spatial distribution of the event in two representative months
243 (June and August), as diagnosed by the different drought indices mention so far.
244 Considering the precipitation deficit (SPEIc), some parts of Europe, including Portugal,
245 northern Italy and eastern Europe experienced severe drought conditions in June, which
246 extended to other regions of France, Germany, the British Islands and northern Spain in
247 August 2022 (Figure 3a). Comparatively, most of the Euro-Mediterranean region was
248 already under severe 12-SPEI conditions by June 2022, and they persisted and extended to
249 the rest of the European continent and northern Africa in August 2022 (Figure 3b). The
250 extreme drought severity in 1-runoff (Figure 3e) and 1-soil moisture (Figure 3f) also
251 exceeded that of the 12-SPEIc (Figure 3a) over most of the Euro-Mediterranean region,
252 demonstrating that AED aggravated the hydrological drought in the summer of 2022.
253 Finally, the resemblance of the 12-SPEI patterns obtained with the temperature-based
254 (observations; Figure 3d) and Penman-Monteith (ERA-land; Figure 3b) AED estimates
255 confirms that the extremely warm temperatures of that summer were the main responsible
256 for the AED increases.

257 The results of this section indicate that the 12-month period in which the 2021/22 Euro-
258 Mediterranean drought reaches its peak depends on the employed index. Since these 12-
259 month periods coincide or vary slightly from the 2021/22 hydrological year (from October
260 2021 to September 2022), the remaining analyses will focus on this time period unless
261 stated otherwise.

262



264 **Figure 3.** Spatial patterns of the different drought indices in June (left) and August (right)
265 2022.

266 **3.2. Atmospheric circulation**

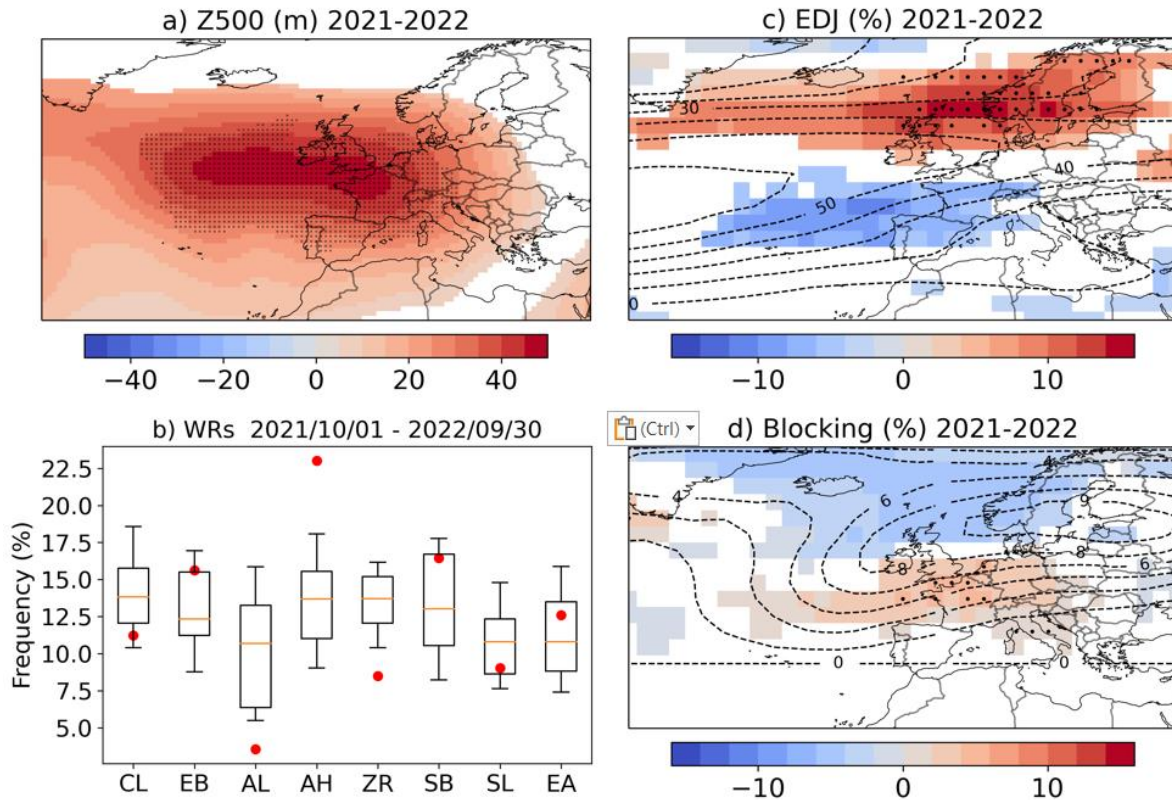
267 To evaluate how anomalous the synoptic conditions were during the 2021/22
268 hydrological year, we computed the anomalies of the annual Z500 with respect to the same
269 period in 1980–2010 (Figure 4a). Significantly positive anomalies occurred over most of
270 Europe (apart from northern Fennoscandia and some easternmost regions), with the largest
271 values located over western Europe and eastern North Atlantic. The magnitude of the Z500
272 anomalies in western Europe was exceptional, exceeding 2.5 standard deviations from the
273 climatology and ranking among the three highest for the 1940–2022 period. This
274 anticyclonic pattern blocked the westerly flow, inducing below-normal rainfall over
275 central/southern Europe, negative anomalies of wind speed in the lower troposphere, and
276 notably, record-breaking anomalies in temperature and solar radiation (Figure S6), in
277 agreement with the elevated AED and unprecedented SPEI values reported in the previous
278 section. The Z500 anomalies suggest an unusual recurrence and/or amplitude of high-
279 pressure systems. To uncover the nature of the atmospheric patterns responsible for these
280 anomalies, we have assessed the frequency of blocking days for the 2021/22 hydrological
281 year. Figure 4d shows the annually averaged percentage of blocking days (contour lines) as
282 well as the anomalies for the 2021/22 hydrological year (shading). Overall, the comparison
283 of the anomalies with the climatology indicates an anomalous southward shift in blocking
284 activity, with a remarkable occurrence of low-latitude blocks. Although canonical high-
285 latitude blocks are traditionally associated with increased precipitation and colder than
286 average temperatures over southern Europe throughout the year, this is not the case for low-

287 latitude blocks, which reduce the odds of heavy precipitation events (Lenggenhager and
288 Martius, 2019; Sousa et al., 2017) and cause extensive above-average temperatures in the
289 area of the anticyclone pattern (Sousa et al. 2018). The centre of Z500 anomalies over
290 western Europe in Figure 4a exhibits a strong spatial overlap with the anomalous blocking
291 patterns, though it also bears some resemblance to subtropical ridges (sometimes referred to
292 as low-latitude blocks; Woollings et al. 2018; Sousa et al. 2021).

293 To address in more detail the type of weather systems behind the low-latitude
294 blocks, we have analysed the annual frequency distribution of the eight daily WRs all year-
295 round (Figure 4b). The fact that three WRs (AL, AH, ZR) show a frequency of occurrence
296 outside the climatological 10–90 percentile range confirms that atmospheric circulation was
297 notably uncommon during the 2021/22 hydrological year. In particular, AH was the
298 dominant atmospheric configuration. Its frequency was record-breaking when compared
299 with the period 1940–2022, almost doubling the climatological average. This result agrees
300 well with the spatial pattern of Z500 anomalies (Figure 4a) and the southward shift in
301 blocking activity (Figure 4d), as AH is characterised by an anticyclonic flow over western
302 Europe (see Figure S3). To provide further insight into whether this pattern exhibits greater
303 coherence with blocks or ridges, we have examined the spatial match between the Z500
304 pattern of the high dominant AH WR and the blocking occurrence during the 2021/22
305 hydrological year. We found that 27.4% of AH days had blocking presence within the
306 region with the largest Z500 anomalies for this WR (30°W–2°E, 45°N–54°N; black box in
307 Figure S3), suggesting that, despite the relatively high contribution of low-latitude blocks,
308 subtropical ridges might have been the main driving force of the AH prevalence during this
309 hydrological year. From a climatological point of view, the WRs leading to the lowest

310 (highest) precipitation over the Euro-Mediterranean region (AH/EB/SB and AL/SL,
311 respectively; see Figure S5) were also the most (least) frequent. The 2021/22 hydrological
312 year had the second-highest frequency of dry WRs (AH+EB+SB) and the third-lowest
313 frequency of wet WRs (AL+SL), agreeing with the observed severity of precipitation
314 deficits reported in the previous section. Hence, and despite the WR variability, the dry
315 conditions of the 2021/22 hydrological year were due, to a large extent, to anomalous
316 atmospheric conditions (i.e. a considerably higher-than-usual frequency of dry WRs).

317 The observed frequencies of AH and low-latitude blocks during the 2021/22
318 hydrological year and their associated rainfall deficits point to a reduced North Atlantic
319 storm track activity, which strongly modulates precipitation over Europe (Hawcroft et al.,
320 2012; Lehmann and Coumou, 2015). An assessment of the North Atlantic EDJ (used as a
321 proxy for storm tracks) during this period shows an enhanced occurrence over the 55°–65°N
322 latitudinal band, being record-breaking over Fennoscandia. This result evidences a
323 poleward shift of the EDJ and associated storm tracks during the 2021/22 hydrological
324 year, as compared to the climatology (Figure 4c). A northward shift implies a lower-than-
325 usual frequency of extratropical cyclones over the Euro-Mediterranean region, in line with
326 the dry conditions experienced during the 2021/22 hydrological year. It also agrees well
327 with the dominance of AH and low-latitude blocks, which tend to accelerate the westerlies
328 in the northern flank of their anticyclonic structure, displacing the climatological position
329 of the EDJ to the pole (e.g., Woollings et al., 2010; Sousa et al. 2018).

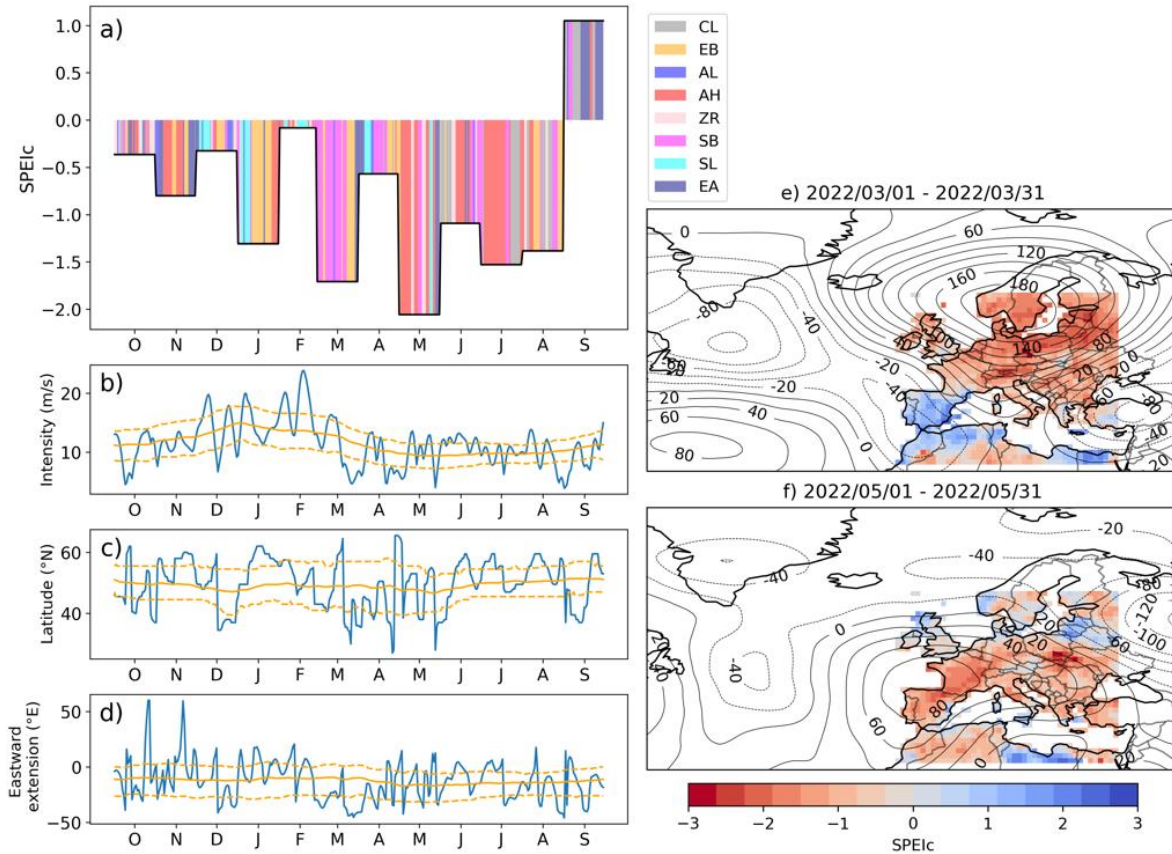


330

331 **Figure 4.** a) Anomalies of year mean 500-hPa geopotential height (Z500; m) during the
 332 hydrological year October 2021 – September 2022 with respect to the climatology (October
 333 1980 – September 2010). Anomalies are shown only when they are significant at the 99.9%
 334 confidence level (two-tailed t-test). Stippling indicates locations where the 2021/22
 335 hydrological year is among the three years with the highest Z500 anomalies for the 1940–
 336 2022 period. b) Frequency distribution of days in each WR for the October 1980 –
 337 September 2010 climatology (boxes). The boxes extend from the lower (Q1) to the upper
 338 (Q3) quartile values of the data, with a horizontal line indicating the position of the median
 339 (Q2). The whiskers extend from the boxes to show the range of the data between the 10th
 340 and 90th percentiles. Red circles correspond to the 2021/22 hydrological year. c-d) As a) but
 341 for the occurrence frequency (%) of the c) EDJ and d) blocking occurrence. The dashed line
 342 contours represent the 1980 – 2010 climatology.

343 All these results provide a robust and consistent picture of the dominant atmospheric
344 circulation signatures associated with the 2021/22 drought at the daily (WR) and weekly
345 (blocking) time scales that are not explicit when we restrict the analysis at the annual scale
346 (Figure 4a). Finally, we describe the evolution of the event through the 2021/22
347 hydrological year to identify the periods that contributed the most to the precipitation
348 deficits. Figure 5a illustrates the daily evolution of WRs (color shading), together with the
349 monthly evolution of the 1-SPEIc from October 2021 to September 2022. As expected, the
350 driest months (lowest 1-SPEIc) are also the ones dominated by dry WRs (warm colors).
351 The most prominent examples occurred in March and May of 2022. March was
352 characterised by a high-latitude blocking pattern (Figure 5e) which was especially
353 persistent, as suggested by the fact that 90% of the days during this month were catalogued
354 as either EB or SB (Table S1). These regimes impeded the normal flow of the westerly
355 winds, leading to a weakening and meandering of the EDJ, with dry conditions in central
356 and northern Europe. The southward displacement of the EDJ favoured precipitation over
357 the Iberian Peninsula, however its eastward extension did not reach the Euro-Mediterranean
358 region (Figure 5b-d), explaining the strong precipitation deficits over central and eastern
359 Mediterranean regions (Figure 5e). May was instead characterised by an extensive
360 anticyclonic pattern over southwestern Europe (Figure 5f), in agreement with the
361 predominance of AH during this month (Table S1). The EDJ was strong and well defined,
362 but it remained slightly above or well below its normal latitude for most of the month
363 (Figure 5b-d). This impeded the passage of the storm track through large parts of the Euro-
364 Mediterranean region, leading to below-normal precipitation therein (Figure 5f).

365 The precipitation deficits during other months of the 2021/22 hydrological year can also be
366 explained by an unusual alternating daily sequence of dry WRs and displaced EDJs. As an
367 illustration, the dry months of January, June, July and August 2023 (all with 1-SPEIc < -1)
368 were characterised by an accumulated monthly frequency of dry EB, AH and SB regimes
369 between 50–75% and a majority of days with northern EDJs (>55°N), far from the drought
370 domain (Figure 5a-d and Table S1). Regarding the summer months (June, July and
371 August), besides lower-than usual precipitation records, high temperatures also played a
372 fundamental role as shown by the considerably higher 1-SPEI as compared to 1-SPEIc (see
373 Table S1). Despite the relatively normal frequency of hot WRs (SB and ZR; see Figure S4)
374 over the Euro-Mediterranean region, the above-average summer temperatures were at least
375 partly due to the near absence of cold WRs (SL and EA). While the accumulated monthly
376 frequency of SB and ZR was between 13–40% for the three months, that of SL and EA was
377 0 for July and August, and 6.7% for June (Table S1). In addition, other WRs leading to
378 regional divergences in temperature anomalies over the Euro-Mediterranean area can help
379 to understand specific heat events at regional level. For instance, the heatwaves of mid-June
380 (ECMWF, 2022) and mid-July (EUMETSAT, 2022) overall coincide with the occurrence
381 of AH, explaining to some extent the high temperatures over southwestern Europe (see
382 Figure S4).



383

384 **Figure 5.** a) Evolution of daily WRs (color shading) and monthly 1-SPEIc derived from
 385 GPCP precipitation and Berkeley temperature (solid black line) during October 2021 –
 386 September 2022. b-d) Daily evolution of EDJ b) intensity (m/s), c) latitudinal position (°N)
 387 and d) eastward extension (°E). The orange solid (dashed) line represents the climatological
 388 values derived from the 31-day moving averages (25 and 75 percentiles) around each
 389 calendar day for the October 1980 – September 2010 climatology. e-f) Monthly anomalies
 390 with respect to the 1980 – 2010 climatology of Z500 (m; contour lines) and 1-SPEIc
 391 (coloured shading) for e) March and f) May 2022, respectively.

392 3.3. Comparison of three major European megadroughts

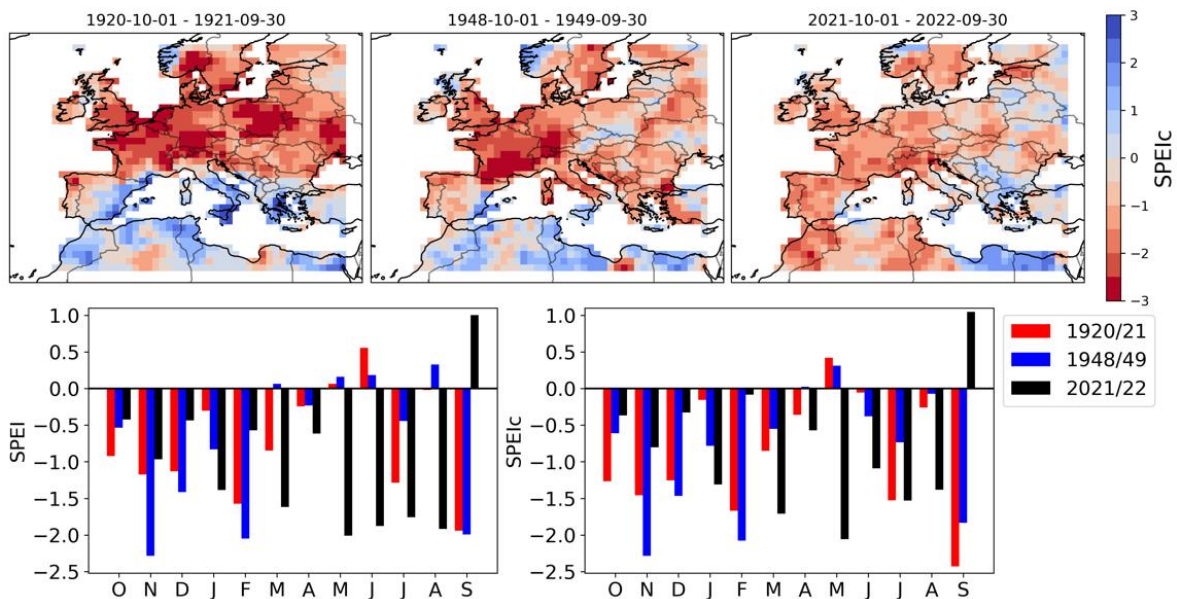
393 We have shown previously that several periods during the 1920s and 1940s were
 394 likely drier than the year 2021/22. This needs to be analysed further and in this section we

395 compare the 2021/22 drought with other major Euro-Mediterranean droughts taking
396 advantage of our long-term series of drought indices (1891–2022). The analysis will be
397 performed for the SPEIc (precipitation deficits) and SPEI (precipitation minus AED)
398 separately. According to the time series of 12-SPEIc, 1948/49 (-2.46), 1920/1921 (-2.45)
399 and 2021/22 (-2.23) were the three driest hydrological years in the Euro-Mediterranean
400 region. For the sake of comparison, Figure 6 shows the spatial pattern of 12-SPEIc (top
401 panels) and the monthly evolution of 1-SPEIc and 1-SPEI (bottom panels) for each of the
402 three drought events, revealing important differences. Unlike the 2021/22 event, the
403 hydrological years of 1920/21 and 1948/49 were relatively wet in the southern regions. The
404 area with negative 12-SPEIc values covered most of the Euro-Mediterranean region during
405 the 2021/22 hydrological year (81.56%), which is slightly larger than in 1920/21 and
406 1948/49 (72.25% and 76.21%, respectively). However, precipitation deficits in 2021/22
407 were not as low as those reached during the other two drought events, particularly over
408 central/western Europe. Accordingly, only 12.86% of the Euro-Mediterranean domain
409 presented severe drought conditions in 2021/22, substantially less than the affected areas in
410 1920/21 and 1948/49 (33.58% and 23.40%, respectively) (Figure 1). We also find
411 important differences in the short-term periods that contributed the most to the 2021/22
412 rainfall deficits as compared to those of 1920/21 and 1948/49 (Figure 6, bottom right
413 panel). The former experienced the driest months during spring and summer (the second
414 half of the hydrological year), whereas the most negative 1-SPEIc values of the two
415 historical events were concentrated throughout autumn and winter months (the first, and
416 typically wetter half of the hydrological year).

417 As discussed in Section 3.1, AED was a decisive component of the 2021/22
418 drought, exacerbating the severity of the event. While the summer of 2022 was record-
419 breaking, 2021/22 experienced the third highest AED over the Euro-Mediterranean region
420 in terms of hydrological year. Interestingly, AED had an opposite effect on the 1920/21 and
421 1948/49 events as compared to 2021/22. Thus, when the AED effects are added up to the
422 SPEI_c, the drought severity (12-SPEI) worsens for 2021/22 (from -2.23 to -2.41) and
423 weakens for 1948/49 (from -2.46 to -1.93) and 1920/1921 (from -2.45 to -1.84). This way,
424 the 2021/22 drought is the most severe of the historical period when the effect of the AED
425 is added to the precipitation. It is worth noticing that the historical SPEI series are derived
426 from temperature-based AED estimates, and hence these differences should be ascribed to
427 temperature effects on AED. In fact, the largest differences between 1-SPEI and 1-SPEI_c
428 for the 2021/22 drought occurred in June (-0.79), August (-0.53) and July (-0.23) of 2022
429 (Table S1 and bottom panels of Figure 6), coinciding with summer record-breaking
430 temperatures over Europe (Copernicus, 2023). These results agree with previous studies
431 reporting that the influence of AED on European droughts has been exacerbated since the
432 1980s as a result of global warming (Stagge et al., 2017). In fact, two attribution studies
433 have already reported the climate change influence on the severity and probability of
434 occurrence of the 2021/22 drought event (Schumacher et al., 2023; Faranda et al., 2023).

435 To illustrate the role of long-term temperature trends in drought severity, we
436 performed an additional exercise. Instead of asking how much weaker the 2021/22 drought
437 could have been in a hypothetical naturalised world, we address the kind of events we could
438 have experienced in the past with the current levels of global warming. To do so, we
439 reconstruct the expected severity of past worst-case events (driven by dramatic but

440 historically plausible precipitation deficits) if they would have occurred under present-day
 441 thermodynamical conditions. The 1920/21 and 1948/49 droughts were both considered for
 442 the construction of worst-case present-day scenarios because of their exceptional severity in
 443 terms of precipitation deficits, and contrasting (mitigating) influences of AED, as compared
 444 to present-day events. To achieve this goal, we have recomputed the 12-SPEI by combining
 445 the observed precipitation deficits during these two historical events with AED estimated
 446 based on the temperatures recorded during the 2021/22 hydrological year. The result shows
 447 that, under present-day conditions, the 1948/49 and 1920/21 hydrological years would have
 448 been much more severe (12-SPEI values of -2.51 and -2.42) than they actually were in the
 449 past (-1.93 and -1.84), and even worse than the 2021/22 event (-2.41). This highlights the
 450 increasing role of AED in drought severity and warns about the current risks of
 451 experiencing unprecedented droughts (even worse than the 2021/22 event). That scenario
 452 would just require that precipitation deficits experienced in the recent past would be
 453 repeated in the present-day climate.



454

455 **Figure 6.** Top panels: Spatial distribution of the 12-SPEIc for the 1920/21, 1948/49 and
456 2021/22 hydrological years. Bottom panels: Evolution of the 1-SPEI (left) and 1-SPEIc
457 (right) for each hydrological year.

458 **4. Discussion and concluding remarks**

459 The 2021/22 hydrological year was characterised by outstanding dry conditions
460 over the Euro-Mediterranean region. In terms of precipitation deficits, most of the region
461 was affected by mild drought conditions and only a few areas experienced severe drought
462 levels. The occurrence of anticyclonic dry weather regimes dominated the atmospheric
463 circulation during this hydrological year, and the observed precipitation deficits are well
464 explained by an unusual recurrence of high-pressure systems over western Europe. This
465 synoptic situation favoured the poleward shift of the North Atlantic eddy-driven jet,
466 decreasing the passage of the storm track over the Euro-Mediterranean region. The
467 prolonged and widespread drought event was also accompanied by exceptionally warm
468 conditions, especially during the summer of 2022. This caused a very important increase in
469 the atmospheric evaporative demand (AED), which led to severe drought conditions (also
470 in terms of runoff and soil moisture) over more than half of the Euro-Mediterranean region.

471 The 2021/22 drought event occurred after a series of intense European droughts
472 associated with precipitation deficits. Some examples are the below-normal rainfall over
473 Iberia during the 2004/05 hydrological year (García-Herrera et al., 2007; Santos et al.,
474 2007), the dry spell in the United Kingdom during the 2010–2012 timeframe (Kendon et
475 al., 2013), the hot and dry summer of 2015 at continental scale (Van Lanen et al., 2016;
476 Ionita et al., 2017; Laaha et al., 2017), and the drought over western and central Europe
477 from July 2016 to June 2017 (García-Herrera et al., 2019). Most of the reported record-

478 breaking droughts use observations from the second half of the 20th century. Nevertheless,
479 when analysed from a long-term perspective, these drought events have not been as
480 extreme as previously perceived both in terms of extension and duration (Hanel et al., 2018;
481 Brázdil et al., 2019; Ionita et al., 2021; Ionita and Nagavciuc, 2021). This stresses the need
482 of long-term observational records to frame better the range of internal variability and the
483 degree of exceptionality of recent droughts in the historical context. In this study, the
484 Standardized Precipitation Evapotranspiration Index (SPEI) and the SPEI with constant
485 AED (SPEI_c) were calculated for the period 1891–2022 over the Euro-Mediterranean
486 region for that purpose.

487 Although the 2021/22 hydrological year was not unprecedented in terms of the
488 precipitation deficits (ranking only below 1948/49 and 1920/21), it has been the most
489 severe drought (SPEI) since at least 1891 as a result of high AED values associated with
490 extreme temperatures. In fact, the 2021/22 hydrological year experienced the third highest
491 AED over the Euro-Mediterranean region, with the summer of 2022 being record-breaking.
492 The severity of the 2021/22 drought event was similar to our current worst-case estimates
493 inferred from observations (i.e. if the driest historical years would have occurred under
494 current temperature conditions). However, these worst-case droughts should be taken as a
495 lower bound (conservative estimates) due to the limited record (unsampled variability) and
496 the ongoing global warming. The 2021/22 drought could thus be viewed as a benchmark
497 and warning of worsening droughts to come in the next decades because of the increase in
498 AED related to global warming.

499 The enhanced AED associated with global warming will aggravate the impacts of
500 droughts, affecting both natural ecosystems (Allen et al., 2015; Williams et al., 2013) and

501 hydrological systems. Although some studies have suggested that the physiological effects
502 related to enhanced CO₂ concentrations could counteract the effects of AED on land
503 evapotranspiration and limit hydrological droughts in the future (Roderick et al., 2015;
504 Scheff, 2018; Yang et al., 2019), the 2021/22 drought is an excellent example of the
505 opposite pattern. Recording an outstanding hydrological drought characterised by reduced
506 soil moisture and very low river discharges under CO₂ concentrations above 400 ppm
507 evidences the fundamental role of the enhanced evapotranspiration, as widely observed
508 during other drought events that have experienced high AED (Zhao et al., 2022). While it is
509 overall clear how climate change affects AED and thus droughts, there is a lot of
510 uncertainty about atmospheric dynamics, which, as we have shown for the 2021/22
511 drought, are also critical to understanding precipitation deficits over the Euro-
512 Mediterranean region. The response of the mid-latitude atmospheric circulation patterns to
513 climate change arises from the competing effects of different remote drivers, including the
514 tropical and polar amplifications, changes in stratospheric vortex strength or the warming
515 of the North Atlantic Ocean (Zappa and Shepherd, 2017; Garrido-Perez et al., 2022).
516 Improving the understanding of these remote driver responses is thus needed to better
517 identify the plausible future evolutions of atmospheric circulation and its associated impact
518 on droughts in the Euro-Mediterranean region.

519 Although we have focused on the 2021/22 hydrological year as an individual event,
520 the consideration of a multi-year perspective also helps to understand the worrisome
521 situation that Europe has been experiencing in recent years. The accumulative effect of
522 multiple consecutive droughts might aggravate the impacts, especially those related to
523 groundwater recharge and forest ecosystems (Moravec et al., 2021, and references therein).

524 Previous studies have already reported that the sequence of recent European droughts is
525 beyond background variability and unprecedented in the observational period (Hari et al.,
526 2020; Büntgen et al., 2021; Moravec et al., 2021; Rakovec et al., 2022). Given the
527 preceding droughts, the occurrence of the 2021/22 drought event might not be considered
528 only as an exceptional individual event, but also as an aggravating factor in an already
529 disturbing hydrological situation, especially if we take into account its magnitude and
530 extent.

531

532 **Acknowledgments**

533 This research work has received support from the European Commission –
534 NextGenerationEU (Regulation EU 2020/2094), through CSIC's Interdisciplinary Thematic
535 Platform Clima (PTI Clima) / Development of Operational Climate Services. SMV-S
536 acknowledges funding by the research projects TED2021-129152B-C41, financed by the
537 Spanish Ministry of Science and FEDER, and MEHYDRO (LINKB20080) financed by the
538 i-LINK 2021 programme of CSIC. RMT was funded by the Portuguese Fundação para a
539 Ciência e a Tecnologia (FCT) I.P./MCTES through national funds (PIDDAC) –
540 UIDB/50019/2020 – Instituto Dom Luiz and project DHEFEUS - 2022.09185.PTDC. We
541 acknowledge the GPCP monthly land-surface precipitation dataset
542 (<https://www.dwd.de/EN/ourservices/gpcp/gpcp.html>) as well as the Berkeley land and
543 ocean temperature dataset (<https://berkeleyearth.org/archive/land-and-ocean-data/>). ERA
544 data products provided courtesy of ECMWF.

545 **References**

- 546 Agnew, C.T., 2000. Using the SPI to Identify Drought. Drought Network News. Accessed
547 at <https://digitalcommons.unl.edu/droughtnetnews/1>
- 548 Allen, C.D., Breshears, D.D., McDowell, N.G., 2015. On underestimation of global
549 vulnerability to tree mortality and forest die-off from hotter drought in the Anthropocene.
550 *Ecosphere* 6, 1–55. <https://doi.org/10.1890/ES15-00203.1>
- 551 Allen, R.G., Pereira, L., Raes, D., Smith, M., 1998. Crop evapotranspiration: guidelines for
552 computing crop water requirements. Food and Agriculture Organization of the United
553 Nations. ISBN 92-5-104219-5
- 554 Ayarzagüena, B., Barriopedro, D., Garrido-Perez, J.M., Abalos, M., de la Cámara, A.,
555 García-Herrera, R., Calvo, N., Ordóñez, C., 2018. Stratospheric Connection to the Abrupt
556 End of the 2016/2017 Iberian Drought. *Geophys. Res. Lett.* 45, 12639–12646.
557 <https://doi.org/10.1029/2018GL079802>
- 558 Bakke, S.J., Ionita, M., Tallaksen, L.M., 2023. Recent European drying and its link to
559 prevailing large-scale atmospheric patterns. *Res. Sq.* [preprint]
560 <https://doi.org/10.21203/rs.3.rs-2397739/v1>
- 561 Barriopedro, D., Ayarzagüena, B., García-Burgos, M., García-Herrera, R., 2022. A multi-
562 parametric perspective of the North Atlantic eddy-driven jet. *Clim. Dyn.*
563 <https://doi.org/10.1007/s00382-022-06574-w>
- 564 Blaney, H., Criddle, W., 1950. Determining water requirements in irrigated areas from
565 climatological and irrigation data. United States Department of Agriculture. SCS TP-96.
- 566 Brázdil, R., Dobrovolný, P., Trnka, M., Řezníková, L., Dolák, L., Kotyza, O., 2019.
567 Extreme droughts and human responses to them: The Czech Lands in the pre-instrumental
568 period. *Clim. Past* 15, 1–24. <https://doi.org/10.5194/cp-15-1-2019>
- 569 Büntgen, U., Urban, O., Krusic, P.J., Rybníček, M., Kolář, T., Kyncl, T., Ač, A., Koňasová,
570 E., Čáslavský, J., Esper, J., Wagner, S., Saurer, M., Tegel, W., Dobrovolný, P., Cherubini,
571 P., Reinig, F., Trnka, M., 2021. Recent European drought extremes beyond Common Era
572 background variability. *Nat. Geosci.* 14, 190–196. <https://doi.org/10.1038/s41561-021-00698-0>
- 574 Cassou, C., 2008. Intraseasonal interaction between the Madden-Julian Oscillation and the
575 North Atlantic Oscillation. *Nature* 455, 523–527. <https://doi.org/10.1038/nature07286>
- 576 Copernicus, 2023. The European State of the Climate 2022. Accessed at
577 <https://climate.copernicus.eu/esotc/2022>
- 578 Davini, P., Cagnazzo, C., Gualdi, S., Navarra, A., 2012. Bidimensional diagnostics,
579 variability, and trends of northern hemisphere blocking. *J. Clim.* 25, 6496–6509.
580 <https://doi.org/10.1175/JCLI-D-12-00032.1>

581 ECMWF, 2022. European heatwaves in June 2022. Accessed at
582 <https://www.ecmwf.int/en/about/media-centre/news/2022/european-heatwaves-june-2022>

583 EUMETSAT, 2022. Heatwaves across Western Europe. Accessed at
584 <https://www.eumetsat.int/heatwaves-across-western-europe>

585 FAO, 2022. Crop Prospects and Food Situation – Quarterly Global Report No. 4, December
586 2022. <https://doi.org/10.4060/cc3233en>

587 Faranda, D., Pascale, S., Bulut, B., 2023. Persistent anticyclonic conditions and climate
588 change exacerbated the exceptional 2022 European-Mediterranean drought. *Environ. Res. Lett.* 18. <https://doi.org/10.1088/1748-9326/acbc37>

590 Fink, A.H., Brücher, T., Krüger, A., Leckebusch, G.C., Pinto, J.G., Ulbrich, U., 2004. The
591 2003 European summer heatwaves and drought –synoptic diagnosis and impacts. *Weather*
592 59, 209–216. <https://doi.org/10.1256/wea.73.04>

593 García-Herrera, R., Garrido-Perez, J.M., Barriopedro, D., Ordóñez, C., Vicente-Serrano,
594 S.M., Nieto, R., Gimeno, L., Sorí, R., Yiou, P., 2019. The European 2016/17 Drought. *J. Clim.* 32, 3169–3187. <https://doi.org/10.1175/jcli-d-18-0331.1>

596 García-Herrera, R., Garrido-Perez, J.M., Ordóñez, C., 2022. Modulation of European air
597 quality by Euro-Atlantic weather regimes. *Atmos. Res.* 277, 1–12.
598 <https://doi.org/10.1016/j.atmosres.2022.106292>

599 García-Herrera, R., Hernández, E., Barriopedro, D., Paredes, D., Trigo, R.M., Trigo, I.F.,
600 Mendes, M.A., 2007. The Outstanding 2004/05 Drought in the Iberian Peninsula:
601 Associated Atmospheric Circulation. *J. Hydrometeorol.* 8, 483–498.
602 <https://doi.org/10.1175/JHM578.1>

603 Garrido-Perez, J.M., Ordóñez, C., Barriopedro, D., García-Herrera, R., Paredes, D., 2020.
604 Impact of weather regimes on wind power variability in western Europe. *Appl. Energy* 264,
605 114731. <https://doi.org/10.1016/j.apenergy.2020.114731>

606 Garrido-Perez, J.M., Ordóñez, C., Barriopedro, D., García-herrera, R., Schnell, J.L.,
607 Horton, D.E., 2022. A storyline view of the projected role of remote drivers on summer air
608 stagnation in Europe and the United States. *Environ. Res. Lett.* 17, 014026.
609 <https://doi.org/10.1088/1748-9326/ac4290>

610 Grams, C.M., Beerli, R., Pfenninger, S., Staffell, I., Wernli, H., 2017. Balancing Europe’s
611 wind-power output through spatial deployment informed by weather regimes. *Nat. Clim. Chang.* 7, 557–562. <https://doi.org/10.1038/NCLIMATE3338>

613 Gudmundsson, L., Seneviratne, S.I., Zhang, X., 2017. Anthropogenic climate change
614 detected in European renewable freshwater resources. *Nat. Clim. Chang.* 7, 813–816.
615 <https://doi.org/10.1038/nclimate3416>

616 Hanel, M., Rakovec, O., Markonis, Y., Máca, P., Samaniego, L., Kyselý, J., Kumar, R.,
617 2018. Revisiting the recent European droughts from a long-term perspective. *Sci. Rep.* 8,
618 1–11. <https://doi.org/10.1038/s41598-018-27464-4>

619 Hargreaves, G.H., Samani, Z.A., 1985. Reference crop evapotranspiration from ambient air
620 temperature. *Appl. Eng. Agric.* <https://doi.org/10.13031/2013.26773>

621 Hari, V., Rakovec, O., Markonis, Y., Hanel, M., Kumar, R., 2020. Increased future
622 occurrences of the exceptional 2018–2019 Central European drought under global
623 warming. *Sci. Rep.* 10, 1–10. <https://doi.org/10.1038/s41598-020-68872-9>

624 Harris, I., Osborn, T.J., Jones, P., Lister, D., 2020. Version 4 of the CRU TS monthly high-
625 resolution gridded multivariate climate dataset. *Sci. Data* 7, 1–18.
626 <https://doi.org/10.1038/s41597-020-0453-3>

627 Hawcroft, M.K., Shaffrey, L.C., Hodges, K.I., Dacre, H.F., 2012. How much Northern
628 Hemisphere precipitation is associated with extratropical cyclones? *Geophys. Res. Lett.* 39,
629 1–7. <https://doi.org/10.1029/2012GL053866>

630 Hersbach, H., Bell, B., Berrisford, P., Hirahara, S., Horányi, A., Muñoz-Sabater, J.,
631 Nicolas, J., Peubey, C., Radu, R., Schepers, D., Simmons, A., Soci, C., Abdalla, S.,
632 Abellan, X., Balsamo, G., Bechtold, P., Biavati, G., Bidlot, J., Bonavita, M., De Chiara, G.,
633 Dahlgren, P., Dee, D., Diamantakis, M., Dragani, R., Flemming, J., Forbes, R., Fuentes,
634 M., Geer, A., Haimberger, L., Healy, S., Hogan, R.J., Hólm, E., Janisková, M., Keeley, S.,
635 Laloyaux, P., Lopez, P., Lupu, C., Radnoti, G., de Rosnay, P., Rozum, I., Vamborg, F.,
636 Villaume, S., Thépaut, J.N., 2020. The ERA5 global reanalysis. *Q. J. R. Meteorol. Soc.* 1–
637 51. <https://doi.org/10.1002/qj.3803>

638 Ionita, M., Dima, M., Nagavciuc, V., Scholz, P., Lohmann, G., 2021. Past megadroughts in
639 central Europe were longer, more severe and less warm than modern droughts. *Commun.*
640 *Earth Environ.* 2, 1–9. <https://doi.org/10.1038/s43247-021-00130-w>

641 Ionita, M., Nagavciuc, V., 2021. Changes in drought features at the European level over the
642 last 120 years. *Nat. Hazards Earth Syst. Sci.* 21, 1685–1701. <https://doi.org/10.5194/nhess-21-1685-2021>

644 Ionita, M., Nagavciuc, V., Kumar, R., Rakovec, O., 2020. On the curious case of the recent
645 decade, mid-spring precipitation deficit in central Europe. *npj Clim. Atmos. Sci.* 3.
646 <https://doi.org/10.1038/s41612-020-00153-8>

647 Ionita, M., Tallaksen, L.M., Kingston, D.G., Stagge, J.H., Laaha, G., Van Lanen, H.A.J.,
648 Scholz, P., Chelcea, S.M., Haslinger, K., 2017. The European 2015 drought from a
649 climatological perspective. *Hydrol. Earth Syst. Sci.* 21, 1397–1419.
650 <https://doi.org/10.5194/hess-21-1397-2017>

651 Jones, D., Brown, S., Czyżak, P., Broadbent, H., Bruce-Lockhart, C., Dizon, R., Ewen, M.,
652 Fulghum, N., Copsey, L., Candlin, A., Rosslowe, C., Fox, H., 2023. European Electricity

653 Review 2023. Accessed at <https://ember-climate.org/insights/research/european-electricity->
654 [review-2023/](https://ember-climate.org/insights/research/european-electricity-review-2023/)

655 Kharrufa, N.S., 1985. Simplified equation for evapotranspiration in arid regions. *Beiträge*
656 *Zur Hydrologie Sonderheft*, 5, 39 – 47.

657 Kendon, M., Marsh, T., Parry, S., 2013. The 2010-2012 drought in England and Wales.
658 *Weather* 68, 88–95. <https://doi.org/10.1002/wea.2101>

659 Kingston, D.G., Stagge, J.H., Tallaksen, L.M., Hannah, D.M., 2015. European-scale
660 drought: Understanding connections between atmospheric circulation and meteorological
661 drought indices. *J. Clim.* 28, 505–516. <https://doi.org/10.1175/JCLI-D-14-00001.1>

662 Laaha, G., Gauster, T., Tallaksen, L.M., Vidal, J.P., Stahl, K., Prudhomme, C., Heudorfer,
663 B., Vlnas, R., Ionita, M., Van Lanen, H.A.J., Adler, M.J., Caillouet, L., Delus, C.,
664 Fendekova, M., Gailliez, S., Hannaford, J., Kingston, D., Van Loon, A.F., Mediero, L.,
665 Osuch, M., Romanowicz, R., Sauquet, E., Stagge, J.H., Wong, W.K., 2017. The European
666 2015 drought from a hydrological perspective. *Hydrol. Earth Syst. Sci.* 21, 3001–3024.
667 <https://doi.org/10.5194/hess-21-3001-2017>

668 Lehmann, J., Coumou, D., 2015. The influence of mid-latitude storm tracks on hot, cold,
669 dry and wet extremes. *Sci. Rep.* 5, 1–9. <https://doi.org/10.1038/srep17491>

670 Lenggenhager, S., Martius, O., 2019. Atmospheric blocks modulate the odds of heavy
671 precipitation events in Europe. *Clim. Dyn.* 53, 4155–4171. [https://doi.org/10.1007/s00382-](https://doi.org/10.1007/s00382-019-04779-0)
672 [019-04779-0](https://doi.org/10.1007/s00382-019-04779-0)

673 Lhotka, O., Trnka, M., Kyselý, J., Markonis, Y., Balek, J., Možný, M., 2020. Atmospheric
674 Circulation as a Factor Contributing to Increasing Drought Severity in Central Europe. *J.*
675 *Geophys. Res. Atmos.* 125, 1–17. <https://doi.org/10.1029/2019JD032269>

676 Michelangeli, P.-A., Vautard, R., Legras, B., 1995. Weather regimes: Recurrence and quasi
677 stationarity. *J. Atmos. Sci.* 52, 1237–1256. [https://doi.org/10.1175/1520-](https://doi.org/10.1175/1520-0469(1995)052<1237:WRRASQ>2.0.CO;2)
678 [0469\(1995\)052<1237:WRRASQ>2.0.CO;2](https://doi.org/10.1175/1520-0469(1995)052<1237:WRRASQ>2.0.CO;2)

679 Moravec, V., Markonis, Y., Rakovec, O., Svoboda, M., Trnka, M., Kumar, R., Hanel, M.,
680 2021. Europe under multi-year droughts: How severe was the 2014–2018 drought period?
681 *Environ. Res. Lett.* 16. <https://doi.org/10.1088/1748-9326/abe828>

682 Muñoz-Sabater, J., Dutra, E., Agustí-Panareda, A., Albergel, C., Arduini, G., Balsamo, G.,
683 Boussetta, S., Choulga, M., Harrigan, S., Hersbach, H., Martens, B., Miralles, D.G., Piles,
684 M., Rodríguez-Fernández, N.J., Zsoter, E., Buontempo, C., Thépaut, J.N., 2021. ERA5-
685 Land: A state-of-the-art global reanalysis dataset for land applications. *Earth Syst. Sci. Data*
686 13, 4349–4383. <https://doi.org/10.5194/essd-13-4349-2021>

687 Oikonomou, P.D., Karavitis, C.A., Tsesmelis, D.E., Kolokytha, E., Maia, R., 2020.
688 Drought Characteristics Assessment in Europe over the Past 50 Years. *Water Resour.*
689 *Manag.* 34, 4757–4772. <https://doi.org/10.1007/s11269-020-02688-0>

690 Peters, W., Bastos, A., Ciais, P., Vermeulen, A., 2020. A historical, geographical and
691 ecological perspective on the 2018 European summer drought: Perspective on the 2018
692 European drought. *Philos. Trans. R. Soc. B Biol. Sci.* 375.
693 <https://doi.org/10.1098/rstb.2019.0505>

694 Rakovec, O., Samaniego, L., Hari, V., Markonis, Y., Moravec, V., Thober, S., Hanel, M.,
695 Kumar, R., 2022. The 2018–2020 Multi-Year Drought Sets a New Benchmark in Europe.
696 *Earth's Futur.* 10, 1–11. <https://doi.org/10.1029/2021EF002394>

697 Roderick, M.L., Greve, P., Farquhar, G.D., 2015. On the assessment of aridity with changes
698 in atmospheric CO₂. *Water Resour. Res.* 51, 5450–5463.
699 <https://doi.org/10.1002/2015WR017031>

700 Rohde, R.A., Hausfather, Z., 2020. The Berkeley Earth Land/Ocean Temperature Record.
701 *Earth Syst. Sci. Data* 12, 3469–3479. <https://doi.org/10.5194/essd-12-3469-2020>

702 Santos, J., Corte-Real, J., Leite, S., 2007. Atmospheric large-scale dynamics during the
703 2004/2005 winter drought in Portugal. *Int. J. Climatol.* 27, 571–586.
704 <https://doi.org/10.1002/joc.1425>

705 Scheff, J., 2018. Drought Indices, Drought Impacts, CO₂, and Warming: a Historical and
706 Geologic Perspective. *Curr. Clim. Chang. Reports* 4, 202–209.
707 <https://doi.org/10.1007/s40641-018-0094-1>

708 Schneider, U., Becker, A., Finger, P., Meyer-Christoffer, A., Ziese, M., Rudolf, B., 2014.
709 GPCP's new land surface precipitation climatology based on quality-controlled in situ data
710 and its role in quantifying the global water cycle. *Theor. Appl. Climatol.* 115, 15–40.
711 <https://doi.org/10.1007/s00704-013-0860-x>

712 Schumacher, D.L., Zachariah, M., Otto, F., Barnes, C., Philip, S., Kew, S., Vahlberg, M.,
713 Singh, R., Heinrich, D., Arrighi, J., van Aalst, M., Hauser, M., Hirschi, M., Bessenbacher,
714 V., Gudmundsson, L., Beaudoin, H. K., Rodell, M., Li, S., Yang, W., Vecchi, G.A.,
715 Harrington, L.J., Lehner, F., Balsamo, G., and Seneviratne, S.I., 2023. Detecting the human
716 fingerprint in the summer 2022 West-Central European soil drought, EGUsphere [preprint],
717 <https://doi.org/10.5194/egusphere-2023-717>

718 Seneviratne, S.I., Zhang, X., Adnan, M., Badi, W., Dereczynski, C., Di Luca, A., Ghosh,
719 S., Iskandar, I., Kossin, J., Lewis, S., Otto, F., Pinto, I., Satoh, M., Vicente-Serrano, S.M.,
720 Wehner, M., & Zhou, B., 2021. Weather and Climate Extreme Events in a Changing
721 Climate. In V. Masson-Delmotte, P., Zhai, A., Pirani, S.L., Connors, C., Péan, S., Berger,
722 N., Caud, Y., Chen, L., Goldfarb, M.I., Gomis, M., Huang, K., Leitzell, E., Lonnoy, J.B.R.,
723 Matthews, T.K., Maycock, T., Waterfield, O., Yelekçi, R., Yu, B. Zhou (Eds.), *Climate*
724 *Change 2021: The Physical Science Basis. Contribution of Working Group I to the Sixth*
725 *Assessment Report of the Intergovernmental Panel on Climate Change* (pp. 1513–1766).
726 Cambridge University Press. <https://doi.org/10.1017/9781009157896.013>

727 Sousa, P.M., Barriopedro, D., García-Herrera, R., Woollings, T., Trigo, R.M., 2021. A new
728 combined detection algorithm for blocking and subtropical ridges. *J. Clim.* 34, 7735–7758.
729 <https://doi.org/10.1175/JCLI-D-20-0658.1>

730 Sousa, P.M., Trigo, R.M., Barriopedro, D., Soares, P.M.M., Ramos, A.M., Liberato,
731 M.L.R., 2017. Responses of European precipitation distributions and regimes to different
732 blocking locations. *Clim. Dyn.* 48, 1141–1160. <https://doi.org/10.1007/s00382-016-3132-5>

733 Sousa, P.M., Trigo, R.M., Barriopedro, D., Soares, P.M.M., Santos, J.A., 2018. European
734 temperature responses to blocking and ridge regional patterns. *Clim. Dyn.* 50, 457–477.
735 <https://doi.org/10.1007/s00382-017-3620-2>

736 Spinoni, J., Naumann, G., Vogt, J. V., 2017. Pan-European seasonal trends and recent
737 changes of drought frequency and severity. *Glob. Planet. Change* 148, 113–130.
738 <https://doi.org/10.1016/j.gloplacha.2016.11.013>

739 Spinoni, J., Naumann, G., Vogt, J. V., Barbosa, P., 2015a. The biggest drought events in
740 Europe from 1950 to 2012. *J. Hydrol. Reg. Stud.* 3, 509–524.
741 <https://doi.org/10.1016/j.ejrh.2015.01.001>

742 Spinoni, J., Naumann, G., Vogt, J. V., Barbosa, P., 2015b. European drought climatologies
743 and trends based on a multi-indicator approach. *Glob. Planet. Change* 127, 50–57.
744 <https://doi.org/10.1016/j.gloplacha.2015.01.012>

745 Stagge, J.H., Kingston, D.G., Tallaksen, L.M., Hannah, D.M., 2017. Observed drought
746 indices show increasing divergence across Europe. *Sci. Rep.* 7, 1–10.
747 <https://doi.org/10.1038/s41598-017-14283-2>

748 Stagge, J.H., Tallaksen, L.M., Gudmundsson, L., Van Loon, A.F., Stahl, K., 2015.
749 Candidate Distributions for Climatological Drought Indices (SPI and SPEI). *Int. J.*
750 *Climatol.* 35, 4027–4040. <https://doi.org/10.1002/joc.4267>

751 Sundström, A., Szeto, S., Fierli, F., 2022. Summer 2022: exceptional wildfire season in
752 Europe. Accessed at [https://www.eumetsat.int/summer-2022-exceptional-wildfire-season-](https://www.eumetsat.int/summer-2022-exceptional-wildfire-season-europe)
753 [europe](https://www.eumetsat.int/summer-2022-exceptional-wildfire-season-europe)

754 Toreti, A., Bavera, D., Acosta Navarro, J., Cammalleri, C., de Jager, A., Di Ciollo, C.,
755 Hrast Essenfelder, A., Maetens, W., Magni, D., Masante, D., Mazzeschi, M., Niemeyer, S.,
756 Spinoni, J., 2022. Drought in Europe August 2022, Publications Office of the European
757 Union, Luxembourg, <https://10.2760/264241>, JRC130493

758 Van Lanen, H.A.J., Laaha, G., Kingston, D.G., Gauster, T., Ionita, M., Vidal, J.P., Vlnas,
759 R., Tallaksen, L.M., Stahl, K., Hannaford, J., Delus, C., Fendekova, M., Mediero, L.,
760 Prudhomme, C., Rets, E., Romanowicz, R.J., Gailliez, S., Wong, W.K., Adler, M.J.,
761 Blauhut, V., Caillouet, L., Chelcea, S., Frolova, N., Gudmundsson, L., Hanel, M.,
762 Haslinger, K., Kireeva, M., Osuch, M., Sauquet, E., Stagge, J.H., Van Loon, A.F., 2016.
763 Hydrology needed to manage droughts: the 2015 European case. *Hydrol. Process.* 30,
764 3097–3104. <https://doi.org/10.1002/hyp.10838>

765 Van Loon, A.F., Tjeldeman, E., Wanders, N., Van Lanen, H.A.J., Teuling, A.J., Uijlenhoet,
766 R., 2014. How climate seasonality modifies drought duration and deficit. *J. Geophys. Res.*
767 119, 4640–4656. <https://doi.org/10.1002/2013JD020383>

768 Van Loon, A.F., Van Lanen, H.A.J., 2012. A process-based typology of hydrological
769 drought. *Hydrol. Earth Syst. Sci.* 16, 1915–1946. [https://doi.org/10.5194/hess-16-1915-](https://doi.org/10.5194/hess-16-1915-2012)
770 2012

771 Vicente-Serrano, S.M., Beguería, S., López-Moreno, J.I., 2010. A multiscalar drought
772 index sensitive to global warming: The standardized precipitation evapotranspiration index.
773 *J. Clim.* 23, 1696–1718. <https://doi.org/10.1175/2009JCLI2909.1>

774 Vicente-Serrano, S.M., López-Moreno, J.I., Beguería, S., Lorenzo-Lacruz, J., Azorin-
775 Molina, C., Morán-Tejeda, E., 2012. Accurate Computation of a Streamflow Drought
776 Index. *J. Hydrol. Eng.* 17, 318–332. [https://doi.org/10.1061/\(asce\)he.1943-5584.0000433](https://doi.org/10.1061/(asce)he.1943-5584.0000433)

777 Vicente-Serrano, S.M., McVicar, T.R., Miralles, D.G., Yang, Y., Tomas-Burguera, M.,
778 2020. Unraveling the influence of atmospheric evaporative demand on drought and its
779 response to climate change. *Wiley Interdiscip. Rev. Clim. Chang.*
780 <https://doi.org/10.1002/wcc.632>

781 Williams, A.P., Allen, C.D., Macalady, A.K., Griffin, D., Woodhouse, C.A., Meko, D.M.,
782 Swetnam, T.W., Rauscher, S.A., Seager, R., Grissino-Mayer, H.D., Dean, J.S., Cook, E.R.,
783 Gangodagamage, C., Cai, M., Mcdowell, N.G., 2013. Temperature as a potent driver of
784 regional forest drought stress and tree mortality. *Nat. Clim. Chang.* 3, 292–297.
785 <https://doi.org/10.1038/nclimate1693>

786 Woollings, T., Barriopedro, D., Methven, J., Son, S.W., Martius, O., Harvey, B., Sillmann,
787 J., Lupo, A.R., Seneviratne, S., 2018. Blocking and its Response to Climate Change. *Curr.*
788 *Clim. Chang. Reports* 4, 287–300. <https://doi.org/10.1007/s40641-018-0108-z>

789 Woollings, T., Hannachi, A., Hoskins, B., 2010. Variability of the North Atlantic eddy-
790 driven jet stream. *Q. J. R. Meteorol. Soc.* 136, 856–868. <https://doi.org/10.1002/qj.625>

791 Yang, Y., Roderick, M.L., Zhang, S., McVicar, T.R., Donohue, R.J., 2019. Hydrologic
792 implications of vegetation response to elevated CO₂ in climate projections. *Nat. Clim.*
793 *Chang.* 9, 44–48. <https://doi.org/10.1038/s41558-018-0361-0>

794 Zappa, G., Shepherd, T.G., 2017. Storylines of atmospheric circulation change for
795 European regional climate impact assessment. *J. Clim.* 30, 6561–6577.
796 <https://doi.org/10.1175/JCLI-D-16-0807.1>

797 Zhao, M.A.G., Liu, Y., Konings, A.G., 2022. Evapotranspiration frequently increases
798 during droughts. *Nat. Clim. Chang.* 12, 1024–1030. [https://doi.org/10.1038/s41558-022-](https://doi.org/10.1038/s41558-022-01505-3)
799 01505-3

Abstract

The Euro-Mediterranean region experienced a remarkable drought during the hydrological year 2021/22. Substantial and widespread impacts on water supply systems, agricultural crops, and the production of hydroelectric power were observed. This assessment characterises the drought from a long-term perspective using a multi-index approach and analyses the associated atmospheric circulation at the annual and monthly time scales. The main dynamical forcing of the drought was the unusual recurrence of high-pressure systems over western Europe, at least partly due to an anomalous southward shift in blocking activity and a remarkable occurrence of low-latitude blocks. This led to record-breaking positive geopotential height anomalies over western Europe and a poleward displacement of the North Atlantic eddy-driven jet. Although most of the region was affected by mild drought conditions, the 2021/22 event was not unprecedented in terms of precipitation deficits since other periods of the 20th century (e.g., in the 1920s, 1940s and 1970s) displayed moderate and severe drought conditions over larger areas. However, the 2021/22 drought has been the most intense since at least 1891 because of high atmospheric evaporative demand (AED) values associated with extreme temperatures, especially during the summer of 2022. This enhanced AED also contributed to depleting soil moisture and reducing runoff generation, leading to unprecedented deficits since at least 1965. Finally, we find important differences in the 2021/22 event as compared to other major historical droughts over the Euro-Mediterranean region. In particular, the contrasting effect of AED evidences its increasing role over the last decades and warns about the current risk of experiencing unprecedented droughts.

Highlights

- Most of the Euro-Mediterranean region affected by drought conditions during 2021/22
- Recursive high-pressure systems & a poleward jet shift explain rainfall deficits
- Most severe drought since at least 1891 when considering evaporative demand (AED)
- Enhanced AED caused unprecedented low soil moisture & runoff since at least 1965
- Potential worst-case droughts if historic rainfall deficits occur with current AED

Declaration of interests

The authors declare that they have no known competing financial interests or personal relationships that could have appeared to influence the work reported in this paper.

The authors declare the following financial interests/personal relationships which may be considered as potential competing interests:



[Click here to access/download](#)

Supplementary material for on-line publication only
Supplementary_JoH.docx



Jose M. Garrido-Perez: Conceptualization, Methodology, Software, Formal analysis, Data curation, Writing – original draft, Visualization. **Sergio M. Vicente-Serrano:** Conceptualization, Methodology, Software, Formal analysis, Data curation, Writing – original draft, Visualization. **David Barriopedro:** Conceptualization, Methodology, Data curation, Writing – review & editing. **Ricardo García-Herrera:** Conceptualization, Methodology, Writing – review & editing. **Ricardo Trigo:** Conceptualization, Methodology, Writing – review & editing. **Santiago Breguería:** Methodology, Writing – review & editing.